ELSEVIER

Journal of Alloys and Compounds 293–295 (1999) 632–636

Journal of ALLOYS AND COMPOUNDS

Contribution of rare-earths to activation property of Zr-based hydride electrodes

X.G. Yang[a,*], Y.Q. Lei[a], K.Y. Shu[a], G.F. Lin[a], Q.A. Zhang[a], W.K. Zhang[b], X.B. Zhang[a], G.L. Lu[c], Q.D. Wang[a]

[a]*Department of Materials Science and Engineering, Zhejiang University, Zhejiang 310027, China*
[b]*Department of Applied Chemistry, Zhejiang University of Technology, Zhejiang 310014, China*
[c]*Central Laboratory, Zhejiang University, Zhejiang 310028, China*

Abstract

The effect of rare earth RE alloying (RE=Ce, Ce-rich mischmetal Mm or La-rich mischmetal Ml) on the crystalline characteristics and electrochemical performances of AB_2 type $(ZrRE)(MnVCrNi)_2$ hydride electrodes was investigated. It is found that RE-alloyed electrodes are activated at the first charge/discharge cycle in comparison with 15 cycles needed to activate RE-free alloys. The electrochemical capacity of the RE modified alloy series studied is also found to increase by about 15%. The RE modification effect on activation has been discussed on the basis of electrochemical impedance spectroscopy (EIS) measurement and XRD analysis.

Keywords: Zr-based electrode; Rare earth metal alloying; Activation; EIS

1. Introduction

AB_2 Laves phase hydride electrodes (i.e. Zr–Cr–Ni and Zr–Mn–Ni based hydrogen storage alloys) have promising electrochemical performances including high discharge capacity, excellent anti-oxidation and thereby high cycling stability etc. for Ni/MH battery application [1], whereas its dense surface oxide protective layer also leads to the poor charging/discharging kinetics and the difficulty in initial activating processes. Recently many researchers are working hard on improving the activation behaviors of the Zr-based AB_2 type Laves phase hydride electrodes by means of surface treatments, which are diversified in principle including the immersion in a dilute HF solution [2], in a strong hot alkaline solution [3] or in an alkaline solution containing some reducing agents [4], the pulverization in hydrogen atmosphere [5], the pre-oxidizing in a hot oxygen atmosphere [6], the anodic polarization [7] or the addition of lanthanum or mischmetals into the alloy [8,9]. All these have been reported to have some positive effects.

Previous studies have revealed that the activation improvement of the rare earth modified alloys results from the precipitation of intermetallics such as LaNi acting as 'active sites' on the surface, although the bulk LaNi alloy itself exhibits no discharge ability at the room temperature in spite of its large hydrogen storage capacity [9]. Others have attributed the improvement to the segregation of rare earth to the surface and subsequent surface cracking due to the volume expansion during the formation of rare earth oxides [8]. The mechanism for activation of the rare earth modified alloys is still in a dilemma. In this investigation, we synthesized RE-modified AB_2 type alloys in the form of $Zr_{0.9}T_{0.1}Mn_{0.5}Cr_{0.10}V_{0.3}Ni_{1.1}$ (T=Ml, Mm or Ce) and investigated the rare earth modification on activation. We also tried to interpret its mechanism from the electrochemistry of phase components.

2. Experimental details

The alloys with compositions $ZrMn_{0.5}Cr_{0.10}V_{0.3}Ni_{1.1}$ and $Zr_{0.9}T_{0.1}Mn_{0.5}Cr_{0.10}V_{0.3}Ni_{1.1}$ (T=Ml, Mm or Ce), were prepared by arc melting under argon atmosphere, with Mm and Ml representing the Ce-rich and La-rich mischmetals respectively. By ICP analysis, the composition of Mm was 34%La, 45%Ce, 5.6%Pr and 18%Nd, and that of Ml 67.8%La, 6.2%Ce, 27.9%Pr and 2.4%Nd. The purity of all constituent metals except Ce (~95%) was all above 99.9%.

*Corresponding author.

0925-8388/99/$ – see front matter
PII: S0925-8388(99)00356-4

The as-cast alloy ingots were crushed mechanically in air. Powder X-ray diffraction data were obtained from sieved grains (−43 μm) of the inactivated alloy using *Rigaku C-max-III B* Diffractometer with a Cu K_α radiation and a nickel diffracted-beam filter.

The hydride electrodes were prepared by cold pressing the mixtures of different alloy powder (−43 μm) with powdered copper (−46 μm) in the weight ratio of 1:2 to form porous pellets of 10 mm diameter. Electrochemical charge–discharge tests were carried out in a trielectrode electrolysis cell, in which the counter-electrode was nickel oxyhydroxide with excess capacity, the reference electrode was Hg/HgO/6M KOH, and the electrolyte was 6M KOH solution. The discharge capacities of hydride electrodes were determined by galvanostatic method reported before [10].

Electrochemical impedance spectroscopy (EIS) measurements were performed on the different hydride electrodes at different activated stages using a Solartron 1250 Frequency Response Analyzer in conjunction with a Solartron 1287 Electrochemical Interface. The voltage perturbation was 10 mV and the frequency region was between 6.5 kHz and 6.5 mHz.

3. Results and discussion

3.1. Electrochemical activation

Fig. 1 shows the initial discharge capacity vs. cycling number of $ZrMn_{0.5}Cr_{0.10}V_{0.3}Ni_{1.1}$ and $Zr_{0.9}T_{0.1}Mn_{0.5}Cr_{0.10}V_{0.3}Ni_{1.1}$ (T=Ml, Mm or Ce) hydrogen storage alloys. The $ZrMn_{0.5}Cr_{0.10}V_{0.3}Ni_{1.1}$ alloy electrode has no ability to discharge proton on the first cycling, and reaches its maximal capacity of 250 mAh g^{-1} at the 14th cycle during its activating process, whereas, the alloys $Zr_{0.9}T_{0.1}Mn_{0.5}Cr_{0.10}V_{0.3}Ni_{1.1}$ (T=Ml, Mm or Ce) all are able to discharge at their maximal capacities of 308, 320 and 356 mAh g^{-1} respectively on the first cycle.

There are two points worthy mentioning. The first is that the rare earth metal Ce or mischmetal alloying can basically solve the problem of activation of $ZrMn_{0.5}Cr_{0.10}V_{0.3}Ni_{1.1}$ alloy electrode. The second, after rare earth alloying, the maximum capacities rise remarkably, from 250 mAh g^{-1} of the mother alloy $ZrMn_{0.5}Cr_{0.10}V_{0.3}Ni_{1.1}$ to 356 mAh g^{-1} of the Ce-containing one. The effect on capacity increments follows the order of Ml<Mm<Ce. A small amount of rare earth metal is found to be able to increase the activation properties of the Zr-based alloy electrodes greatly. In another word, the A-side metal elements have predominant influence on the electrochemical performances of AB_2 alloys. In order to assure good activation of Zr-based hydride electrodes, it is worthy to find suitable composition for A-side elements.

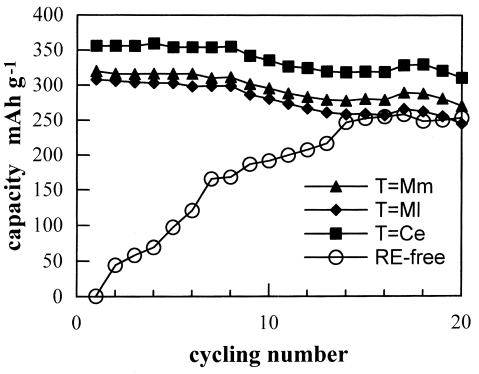

Fig. 1. The activation processes of $Zr_{0.9}T_{0.1}Mn_{0.5}Cr_{0.10}V_{0.3}Ni_{1.1}$ (T=Ml, Mm or Ce) hydrogen storage alloys in comparison with that of $ZrMn_{0.5}Cr_{0.10}V_{0.3}Ni_{1.1}$ (○), at 50 mA g^{-1} and T=298 K.

3.2. XRD analyses

Fig. 2 shows the XRD patterns of $Zr_{0.9}T_{0.1}Mn_{0.5}Cr_{0.10}V_{0.3}Ni_{1.1}$ (T=Zr, Ml, Mm or Ce) as-cast alloys. The main phase of $ZrMn_{0.5}Cr_{0.10}V_{0.3}Ni_{1.1}$ alloy is found to be C15 type, and its lattice parameter (a) equals to 0.7064 nm. Small amount of C14 phase and pseudo-binary ZrNi type alloy were also detected in the RE-free alloy [1].

After RE modification, the $Zr_{0.9}T_{0.1}Mn_{0.5}Cr_{0.10}V_{0.3}Ni_{1.1}$ (T=Ml, Mm or Ce) alloys all have the same dominant phase C15, with lattice parameters almost the same. However, the content of C14 phase rises, and its lattice constants also expand to some extend. It is believed that RE atoms dissolve into the C14 phase. Because of the mismatch in atomic sizes of RE and Zr, the RE substitution induces a distorted C14 lattice structure. The energy required for hydrogen atom to enter or get out distorted tetrahedral interstices is generally lower. By SEM and TEM analyses, C14 phase is found to precipitate dispersively in the C15 dentritic matrix with a definite crystalline

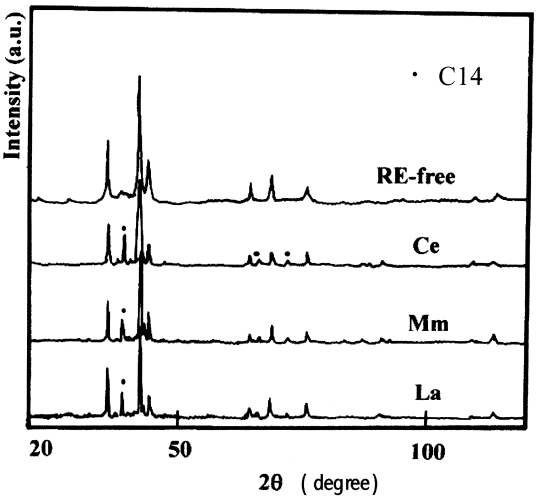

Fig. 2. XRD patterns of $Zr_{0.9}T_{0.1}Mn_{0.5}Cr_{0.10}V_{0.3}Ni_{1.1}$ (T=Zr, Ml, Mm or Ce) as-cast hydrogen storage alloys.

orientation relationship [10], i.e. $(0001)_{C14}//\{111\}_{C15}$ and $\langle 1\bar{2}10\rangle_{C14}//\langle 1\bar{1}0\rangle_{C15}$. Lattice strain expands from their phase boundary into core regions of crystals (C14 and C15). These crystalline features would modify thermodynamic and kinetic properties of the RE modified alloys.

3.3. Electrochemical impedance spectroscopy

Electrochemical impedance spectroscopy (EIS) was applied to study the RE-free and RE-alloyed metal hydride electrodes. Fig. 3 depicts the Nyquist plots of $Zr_{0.9}T_{0.1}Mn_{0.5}Cr_{0.10}V_{0.3}Ni_{1.1}$ (T=Zr, Ml, Mm or Ce) alloy electrodes, which are first charged for 4.0 h at 100 mA g^{-1}. All studied hydride electrodes display two EIS semicircles. The smaller semicircle in the high-frequency region is related to the resistance and capacitance between the current collector and the pellets of alloy powders. The larger semicircle in the low-frequency region is related to the electrochemical reaction and the double-layer capacitance on the alloy particles [11]. The front smaller semicircles related to the contact resistance in all electrodes are the same, indicating that there is no obvious difference in contact resistance among the different electrodes. This result backs up our previous viewpoint that the semicircular in high-frequency region is attributed to contact resistance.

The semicircle in the low-frequency region is much larger for RE-free electrode than for RE-alloyed electrodes. The Ce (or Ce-rich mischmetal) alloying electrode has the smallest high-frequency semicircle indicating the lowest reaction resistance (about 11.7 Ω obtained by simulation). The low electrochemical reaction resistance makes the RE modified electrodes activated easily. The Ce substituting greatly reduces the overpotential for charge/discharge reaction as well.

For RE-free electrode, the larger reaction resistance (about 48.6 Ω) brings forth the lower charging efficiency in the initial cyclings, which makes the RE-free electrode unable to be saturated with protons during charging process. Meanwhile, a larger resistance in the RE-free electrode also results in a higher anodic potential, which makes the electrode potential drop rapidly to the cut-off potential and hence incomplete hydrogen discharging, which retardates the activation process.

Fig. 4 shows the Nyquist plots of $Zr_{0.9}T_{0.1}Mn_{0.5}Cr_{0.10}V_{0.3}Ni_{1.1}$ (T=Zr, Ml, Mm or Ce) fully activated electrodes in 85% state of charge, and Fig. 5 shows those discharged to −0.6 V vs. Hg/HgO. As can be seen in Fig. 4, the salient change is that the total resistance of the four electrodes reduces markedly compared to that in Fig. 3. The semicircles at high frequencies change very little, this implies that contact resistance in all electrodes does not change obviously even after activation. This phenomenon also can help to clear out the argument in the debate that the semicircular curve in the high frequency region reflects to the contact resistance and capacitance, because only the electrochemical reaction would improve greatly after activation. So the semicircles in the high frequency range in the Nyquist plot stand for the contact resistance instead of the resistance in electrochemical reaction.

The activated electrode modified with Ce or Ce-rich Mm has almost the same reaction resistance (2.52 Ω). The reaction resistance for the RE-free electrode is reduced to 4.17 Ω in comparison with that (48.6 Ω) in Fig. 3. The reaction resistance of the Ml modified electrode is very close to that of the RE-free one.

In Fig. 5, all electrodes have been discharged to the cut-off potential −0.6 V, therefore very low hydrogen concentration. The Ce-containing electrode has the lowest

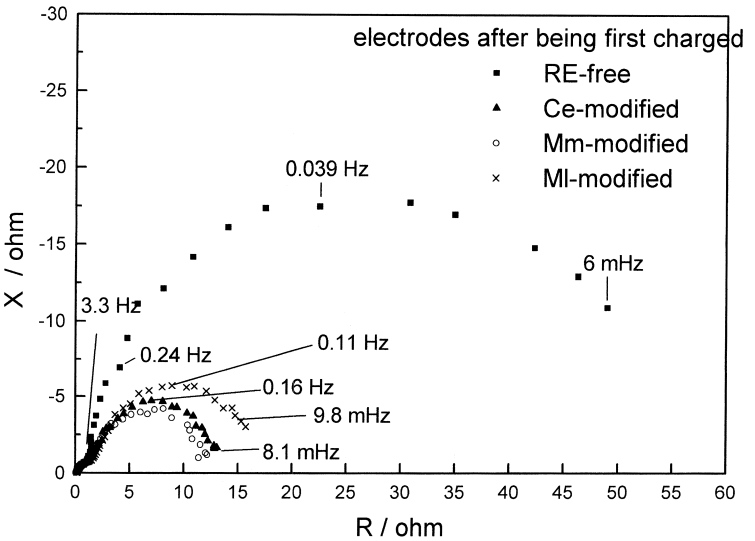

Fig. 3. The Nyquist plots of $Zr_{0.9}T_{0.1}Mn_{0.5}Cr_{0.10}V_{0.3}Ni_{1.1}$ (T=Zr, Ml, Mm or Ce) alloy electrodes which are all first charged for 4.0 h at 100 mA g^{-1}.

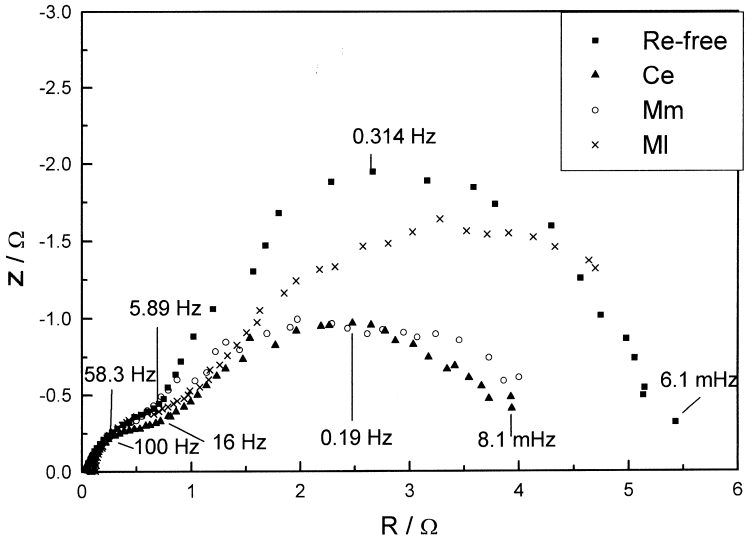

Fig. 4. The Nyquist plots of $Zr_{0.9}T_{0.1}Mn_{0.5}Cr_{0.10}V_{0.3}Ni_{1.1}$ (T=Zr, Ml, Mm or Ce) activated electrodes in 85% state of charge.

hydrogen concentration since the amount of hydrogen discharged from it is the largest, with the initial hydrogen capacities for all electrodes almost the same. This fact is also verified by the appearance of the Warburg line, which is attributed to the hydrogen diffusion in the electrode, instead of a low-frequency semicircle as shown in Fig. 5. Since the Ce-containing electrode has good electrochemical reactivity that deepens its discharge depth and lowers hydrogen content in the electrode, its anodic polarization mainly results from hydrogen diffusion, which becomes the rate limiting factor, when the electrode is discharged to cut-off potential.

In the EIS of La-modified electrode, the lower frequency semicircle is larger and more depressed than that of other electrodes, which implies that La or its compound (oxide, hydroxide etc.) makes the reaction resistance much higher than that of the Ce-alloyed electrodes. Meanwhile the depressed shape reflects that the lanthanum compounds on the surface elevate the capacitance component.

4. Conclusions

It was found that RE-alloyed electrodes $(ZrRE)(MnVCrNi)_2$ were activated at the first charge/discharge cycle in comparison with 15 cycles needed to activate a RE-free alloy electrode. The electrochemical capacity of the studied RE modified alloy series was also

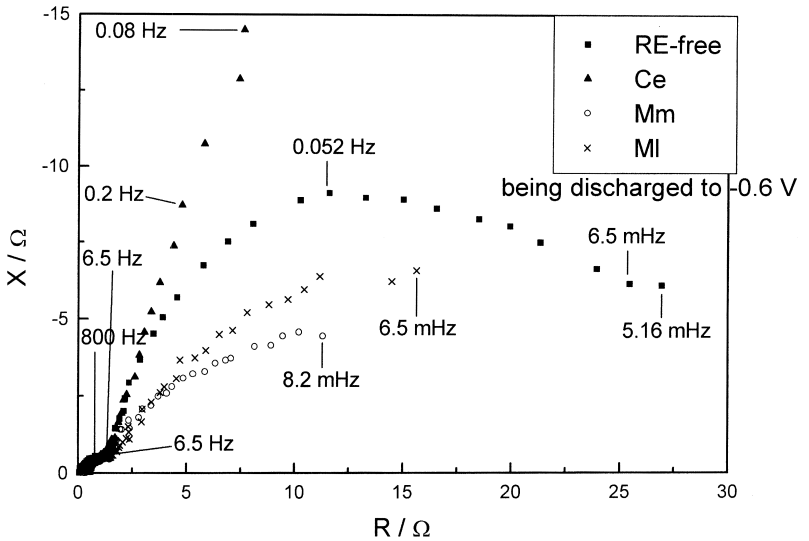

Fig. 5. The Nyquist plots of $Zr_{0.9}T_{0.1}Mn_{0.5}Cr_{0.10}V_{0.3}Ni_{1.1}$ (T=Zr, Ml, Mm or Ce) activated electrodes which are discharged to −0.6 V vs. Hg/HgO.

found to increase by about 15%. EIS study indicates that the improvement in activation can be mainly attributed to the lower reaction resistance caused by RE modification. For RE alloying, the Ce substitution exhibits a more effective reduction in the overpotential for charge/discharge reaction and higher activation than the La-rich mischmetal substitution. XRD analysis reveals that the main phase C15 and its lattice parameter do not change after RE alloying, whereas C14 phase abundance and its lattice constants are increased. It is believed that RE atoms dissolve into the C14 phase and induce a distorted C14 lattice structure. Because C14 phase dispersively precipitates in the C15 matrix with a definite crystalline orientation relation, distortion stress expands into the C15 main phase along the phase boundaries and improves the activation property of the alloy.

Acknowledgements

This work is supported by National ‘‘863’’ Program and National Natural Science Foundation of China (59601006 and 59671016).

References

[1] X.G. Yang, Y.Q. Lei, W.K. Zhang, G.M. Zhu, Q.D. Wang, J. Alloys Comp. 243 (1996) 151.
[2] A. Zuttel, F. Meli, L. Schlapbach, J. Alloys Comp. 209 (1994) 99.
[3] Y. Yan, G. Sandrock, S. Suda, J. Alloys Comp. 216 (1994) 237.
[4] C. Iwakura, I. Kim, N. Matsui, H. Inoue, M. Matsuoka, Electrochem. Acta 40 (1995) 561.
[5] Y. Moriwaki, T. Gamo, A. Shintani, T. Iwaki, Denki Kagaku 57 (6) (1989) 839.
[6] H. Sawa, M. Ohta, H. Nakano, S. Wakao, Z. Phys. Chem. 164 (1989) 1527.
[7] S. Wakao, H. Sawa, J. Less-Common Met. 172–174 (1991) 1219.
[8] S.R. Kim, J.Y. Lee, J. Alloys Comp. 185 (1992) L1.
[9] D.L. Sun, M. Latroche, A. Percheron-Gugean, J. Alloys Comp. 248 (1997) 215.
[10] X.Y. Song, Y.Q. Lei, X.B. Zhang et al., Proc. of Int. 7th Beijing Conf. and Exhib. on Instrum. Analysis, Shanghai, 1997, P A93.
[11] N. Kuriyama, T. Sakai, H. Miyamura, I. Uehara, H. Ishikawa, T. Iwasaki, J. Alloys Comp. 202 (1993) 183.